

**Controlled Spatial distribution of functional units in the two dimensional nanospace of layered silicates and titanates**

Journal:	<i>Dalton Transactions</i>
Manuscript ID:	DT-PER-01-2014-000147.R1
Article Type:	Perspective
Date Submitted by the Author:	25-Mar-2014
Complete List of Authors:	Ogawa, Makoto; Waseda University, Department of Earth Sciences Saito, Kanji; Waseda University, Graduate School of Creative Science and Engineering Sohmiya, Minoru; Waseda University, Department of Earth Sciences

PERSPECTIVE

Controlled spatial distribution of functional units in the two dimensional nanospace of layered silicates and titanates

Cite this: DOI: 10.1039/x0xx00000x

Makoto Ogawa^{*a,b}, Kanji Saito^b and Minoru Sohmiya^{a,b}Received 00th January 2012,
Accepted 00th January 2012

DOI: 10.1039/x0xx00000x

www.rsc.org/

The immobilization of functional units in the interlayer spaces of layered silicates and titanates is summarized from the viewpoints of how spatial distribution of functional units in the interlayer affects the performance of the intercalation compounds. The ways of incorporating controlled amounts of functional units with controlled spatial distribution are also discussed. As a result of controlled spatial distribution of functional units in two-dimensional nanospace, one can achieve improved efficiency of photo-induced events (photoluminescence and photoinduced electron/energy transfer), molecular sieving and substrate/product selective catalytic reaction.

Contents

1. Introduction
2. Ionic guest
 - 2-1. Ion exchange and characterization
 - 2-2. Effects of the spatial distribution of guest on the function of intercalation compounds
3. Covalent attachments of functional units
4. Hierarchically designed hybrid structures
5. Conclusions and future perspectives

1. Introduction

The spatial distribution and mobility of functional units on solid surfaces are key issues for constructing functional hybrid materials. One can imagine the importance of the spatial distribution of functional units from the beautiful nanostructures of natural organisms, *i.e.* photosynthesis, as well as the useful phenomena achieved in various artificial systems.¹ In solutions, dissolved species distribute homogeneously, while in solid-state host–guest systems, the distribution of guest species is not simple; anisotropic and in some cases more heterogeneous. The structural and chemical homogeneity of hosts is a basic prerequisite to design the spatial distribution of guest species. In addition, the host–guest interactions, the guest–guest interactions and the free space for guest species should be concerned for the spatial distribution and mobility of functional units.²

Among available host–guest systems, intercalation of guest species into layered inorganic solids is a way of constructing two-dimensionally ordered inorganic-organic assembly with unique microstructures controlled by host–guest and guest–guest interactions.^{2–9} One of the most important characteristics of intercalation chemistry is the expansion of the interlayer space upon intercalation of guest species. The expanded space can be used to immobilize guest species further. This ‘*one dimensionally expandable 2-dimensional nano-space*’ is regarded as a nano-vessel or nano-reaction environment for various kinds of molecular species. The properties of intercalation compounds are affected by the population (or density or distance) of functional units and novel function can be emerged only when appropriate population (nanostructure) is achieved. In addition to the density of functional units in each interlayer space, the location of guest species at the external surface of layered compounds (not interlayer space) is possible and the externally adsorbed species may contribute the modification of materials’ performances.

In the present review article, we will discuss how the spatial distribution of guest species affects the performance of the intercalation compounds of layered silicates and titanates. The controlled spatial distribution of functional units has been achieved so far mainly on the host–guest systems based on grafting and cation exchange, so we will focus on such host–guest systems in this article. In addition, the way to immobilize functional units with controlled spatial distribution will also be discussed from the synthetic chemistry viewpoints.

2. Ionic Guests

2-1. Ion exchange and characterization

Layered inorganic solids with varied composition and structures are available,²⁻⁵ many of them are cation exchangeable. One of the most famous examples to show the importance of layer charge density of ion exchangeable layered solids is 2:1 type layered clay minerals (or mica-type layered silicate). Starting from the layered structure of talc and pyrophyllite, depending on the amount of isomorphous substitution in the silicate layer, layered clay minerals with different interlayer reactivity for intercalation are present (Fig. 1).^{3, 8-10} It is impossible to intercalate cationic guest species into the interlayer spaces of talc and pyrophyllite, because there are no layer charges in their structures. The isomorphous substitution of framework elements with lower balance ion ($\text{Si}^{4+} \rightarrow \text{Al}^{3+}$, $\text{Al}^{3+} \rightarrow \text{Mg}^{2+}$, $\text{Mg}^{2+} \rightarrow \text{Li}^+$ etc.) generates negative charge on the silica layer, consequently cation exchangeable solids form. The general chemical formula of smectite is given as $(\text{M}^{x+y} \cdot n\text{H}_2\text{O})(\text{R}^{3+}_{2-y}\text{R}^{2+}_y)(\text{Si}_{4-x}\text{Al}_x)\text{O}_{10}(\text{OH})_2$ (di-type) or $(\text{M}^{x+y} \cdot n\text{H}_2\text{O})(\text{R}^{2+}_{3-y}\text{R}^{3+}_y)(\text{Si}_{4-x}\text{Al}_x)\text{O}_{10}(\text{OH})_2$ (tri-type) (R^{2+} , R^{3+} are the generic divalent and trivalent octahedral cation, respectively; and M^+ is the generic monovalent interlayer cation), where the amount of the interlayer exchangeable cation, which compensates net negative charge of silicate layer, corresponds to the cation exchange capacity of ca. 70-100 milliequivalent / 100 g of clay (meq./100 g of clay). With larger degree of isomorphous substitution, the cation exchange capacity (abbreviated as CEC) becomes larger. Vermiculite (with the ideal chemical formula of $(\text{M}^{x+y}(\text{Al}_{2-y}\text{Mg}_y)(\text{Si}_{4-x}\text{Al}_x)\text{O}_{10}(\text{OH})_2$ (di-type) or $\text{Mg}^{2+}_{(x-y)/2}(\text{Mg}_{3-y}\text{M}^{3+}_y)(\text{Si}_{4-x}\text{Al}_x)\text{O}_{10}(\text{OH})_2$ (tri-type)) is another type of 2:1 type layered silicate and their cation exchange capacity is ca. 250 meq./100 g of clay. Though vermiculite is an ion exchanger with large CEC, which is advantageous for the application to concentrate larger amount of cationic species, the ion exchange requires longer period and severe conditions if compared with the ion exchange of smectites, which is important drawback for the application as an ion exchanger. Mica is another type of 2:1 type layered silicate, where the amounts of interlayer cation (basically K^+) is much larger (the chemical formula can be expressed as $\text{K}^{x+y}(\text{R}^{3+}_{2-y}\text{R}^{2+}_y)(\text{Si}_{4-x}\text{Al}_x)\text{O}_{10}(\text{OH}, \text{F})_2$ (di-type) or $\text{K}^{x+y}(\text{R}^{2+}_{3-y}\text{R}^{3+}_y)(\text{Si}_{4-x}\text{Al}_x)\text{O}_{10}(\text{OH}, \text{F})_2$ (tri-type)) than those of vermiculites and smectites. Due to the large amount of interlayer cations and the strong interactions between interlayer potassium ion and the hexagonal hole located on the silicate layer surface, it is difficult or impossible to replace the interlayer K^+ of mica, therefore mica is not regarded as a cation exchanger. Thus, the CEC value is very important to determine the ion exchange reaction; capacity, selectivity and rate, in addition to the properties of the ion exchanged products.

Efforts have been made to synthesize smectite type layered silicates for possible applications.^{11, 12} Synthesizing smectites analogues has advantages; when the pure smectites with desired

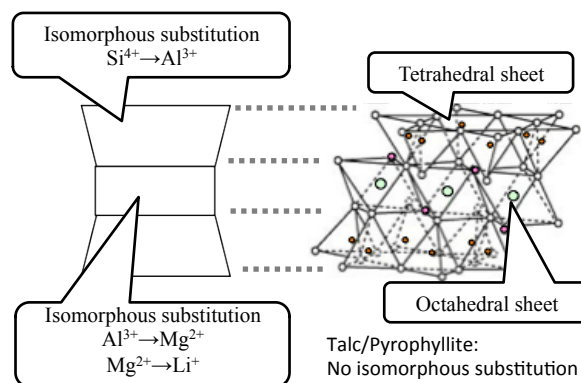


Fig. 1 Schematic drawings of the structure of 2:1 type layer silicates

composition were obtained, one can avoid the problems associated with contamination associated. There are several reports on the controlled layer charge density of synthetic smectites.^{11, 12} Hofman-Klemen effect,¹³ which is a phenomenon of penetrating such interlayer cation as Li^+ into a vacancy of the silicate layer to modify the net negative charge of the layer by moderate thermal treatment, has been discovered and applied to reduce the layer charge density.^{14, 15}

As analogous 2:1 type layered silicates, so-called "Fluorine micas", in which hydroxyl groups are replaced with fluorine groups, are known.^{16, 17} Taeniolite, tetrasilicic mica and fluorine hectorite are examples of commercially available materials with the layer charge density corresponds to vermiculites and smectites. Thus, 2:1 type layered silicates with varied layer charge density are available.

Hydroxyl bearing layered solids such as layered silicates, titanates and niobates are also known as cation exchangeable layered solids. Layered alkali silicates are characterized by the interlayer hydroxyl groups, which play important roles on ion exchange and grafting.^{3, 18, 19} The cation exchange capacity of such layered materials is determined by the density of hydroxyl group on the layer surface.^{3, 18} Due to the origin of the cation exchange mechanism, the quantitative cation exchange depends on the pH of the reaction media, while, to the best of our knowledge, there are no reports on the ion exchange with semi-quantitative amount of cations without segregation. Layered alkali silicates such as kanemite ($\text{NaHSi}_2\text{O}_5 \cdot n\text{H}_2\text{O}$), octosilicate ($\text{Na}_8\text{Si}_{32}\text{O}_{64}[\text{OH}]_8 \cdot 32\text{H}_2\text{O}$), magadiite (the ideal formula is $\text{Na}_2\text{Si}_{14}\text{O}_{29} \cdot 10\text{H}_2\text{O}$) and kenyaite ($\text{Na}_2\text{Si}_{22}\text{O}_{45} \cdot 11\text{H}_2\text{O}$) are an interesting class of layered solids.³ The layer thickness of these silicates were 0.49 (kanemite), 0.63 (octosilicate), 1.12 (magadiite) and 1.49 nm (kenyaite), while the layer charge density seems to be similar. One unique application of the four silicates is to examine the possible communication between adjacent probes across the layer. The spatial distribution of functional units in the two dimensional nanospaces affects the physicochemical properties of the products. On the other hand, the communication between adjacent guest species in the direction perpendicular to the layer (through the layer) has never been discussed. We have reported the possible three-dimensional distance control of functional

	Structure	Thickness of layer nm	Ideal cation exchange capacity meq. g ⁻¹	Layer charge density nm ² e ⁻¹
Kenyaite Na ₂ Si ₂₂ O ₄₅ · 10H ₂ O		1.64	1.36	0.26
Magadiite Na ₂ Si ₁₄ O ₂₉ · 9H ₂ O		1.12	2.0	0.26
Octosilicate Na ₈ [Si ₃₂ O ₆₄ (OH) ₈ · 32H ₂ O]		0.74	2.8	0.26
Kanemite NaHSi ₂ O ₅ · 3H ₂ O		0.49	4.7	0.18

Fig. 2 Structures of a series of layered alkali silicates; kanemite, makatite, octosilica, magadiite and kenyaite

units using these layered silicates with variable layer thickness and europium ions as a photoluminescent probe.²⁰

The preparation, structure and properties of a number of such layered alkali-metal titanates as K₂Ti₂O₅,²¹ Na₂Ti₃O₇,²² K₂Ti₄O₉,²³ and Cs₂Ti₅O₁₁²⁴ have been reported. Among available layered transition metal oxide salts, lepidocrocite-type layered titanates are quite useful as functional materials, because the substitution of the titanate layer is possible to vary the layer charge density. In comparison with other layered alkali titanates (K₂Ti₂O₅, Na₂Ti₃O₇, K₂Ti₄O₉, and Cs₂Ti₅O₁₁), lepidocrocite-type layered titanates (general formula of A_xTi_{2-y}M_yO₄; A, interlayer cation; M, metal ion or vacancy) possess relatively simple structure; the layer is composed of edge-shared TiO₆ octahedrons and the surface is flat compared with those of corrugated layers of K₂Ti₂O₅ composed of a pair of TiO₅ trigonal bipyramid or Na₂Ti₃O₇, K₂Ti₄O₉ and Cs₂Ti₅O₁₁ by being stepped every three, four and five TiO₆ octahedrons, respectively. Some of the interlayer alkali metal ions of A_xTi_{2-y}M_yO₄ compensate the negative charge of the titanate layer, which arises from the substitution of lower valence metal or vacancies for Ti (Fig. 3).

Lepidocrocite-type layered titanates were first described by Reid *et al.*,²⁵ who prepared Rb_xMn_xTi_{2-x}O₄ (0.60 < x < 0.80) by a solid-state reaction between RbMnO₄ and TiO₂ and showed the structure related to lepidocrocite, γ-FeO(OH); Mn(III) and Ti(IV) occupy the Fe sites, O occupies the O and (OH) sites and Rb ions are located between the manganese titanate sheets, balancing the negative charge generated by the replacement of Ti(IV) with Mn(III). Raveau *et al.* have extended the structure type of Rb_xMn_xTi_{2-x}O₄ to a wide variety of analogous compounds, Cs_xTi_{2-x/4}□_{x/4}O₄ (0.58 ≤ x ≤ 0.90, □ = vacancy),²⁶ K_xM_yTi_{2-y}O₄ (M = Mg, Co, Ni, Cu, Zn, Mn, Fe, *etc.*), 0.70 ≤ x ≤ 0.90,²⁵ prepared by solid-state reaction of Cs₂CO₃-TiO₂ system

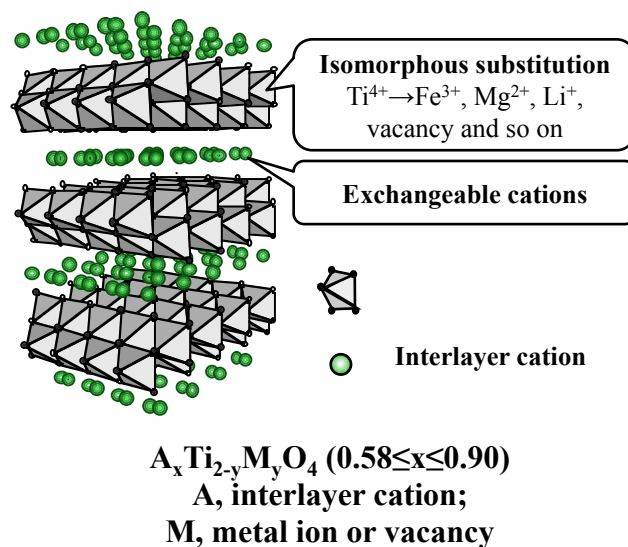


Fig. 3 Crystal structure of lepidocrocite-type layered titanate

and K₂CO₃-metal oxides-TiO₂ system, respectively. Grey *et al.* investigated the preparation and structure of Cs_xTi_{2-x/4}□_{x/4}O₄ in more detail.^{25, 27}

Sasaki *et al.* have extensively investigated the reactivity of Cs_xTi_{2-x/4}□_{x/4}O₄.²⁸⁻³⁰ Among four layered protonic titanates (H₂Ti₃O₇, H₂Ti₄O₉, H₂Ti₅O₁₁ and H_xTi_{2-x/4}□_{x/4}O₄ (x = ca. 0.7)), pyridine was intercalated only into H_xTi_{2-x/4}□_{x/4}O₄. They speculated that the lowest layer charge density was a reason for the difference although several factors, such as acidity, might also be concerned.³⁰ Sasaki found the exfoliation (non-limited swelling) of H_xTi_{2-x/4}□_{x/4}O₄ in aqueous tetrabutylammonium hydroxide solution and the exfoliated H_xTi_{2-x/4}□_{x/4}O₄ was termed as “nanosheet” or “exfoliated nanosheet”.³¹⁻³³ They have also investigated the syntheses of novel lepidocrocite-type layered titanates containing various heteroelements in the titanate layer as well as the interlayer exchangeable cation. A_xTi_{2-x/3}Li_{x/3}O₄ (A = K, Rb and Cs; x = 0.80 for A = K, 0.75 for Rb and 0.70 for Cs, respectively) has been synthesized by solid-state reaction of alkali metal carbonates and TiO₂.³⁴ The single crystal of K_{0.8}Ti_{1.73}Li_{0.27}O₄ with the lateral size of over 1 mm was obtained via a melt and recrystallization process in a K₂MoO₄ flux (TiO₂-K₂CO₃-LiCO₃-MoO₃ system).³⁵ The compositional versatility is one of the most notable characteristics of lepidocrocite-type layered titanates, leading to the electronic, optical and catalytic properties controlled by the introduction of heteroelements in the sheet. Recently, Osada *et al.* have reported that Ti_{0.8}Co_{0.2}O₂ derived from the exfoliation of K_{0.8}Ti_{1.6}Co_{0.4}O₄ shows ferromagnetism even at room temperature.^{36, 37} Fe-substituted lepidocrocite-type layered titanates, such as K_{0.8}Fe_{0.8}Ti_{1.2}O₄, have a potential as photocatalysts under visible light irradiation.³⁸

Yamanaka *et al.* reported the control of layer charge density of Rb_xMn_xTi_{2-x}O₄ via the oxidation of Mn³⁺ to Mn⁴⁺.³⁹ By the oxidation of Rb_xMn_xTi_{2-x}O₄ (x = 0.75) with aqueous sulfonic acid containing Ce(SO₄)₂, Rb_xMn_xTi_{2-x}O₄ with the smaller Rb⁺ content (corresponds to the amount of Mn³⁺ oxidized to Mn⁴⁺)

formed depending on the amount of the added $\text{Ce}(\text{SO}_4)_2$. The Rb^+ content was reduced down to 0.43, which was smaller than the smallest value (0.60) reported by the solid-state synthesis.²⁵ The basal spacing of the oxidized $\text{Rb}_x\text{Mn}_x\text{Ti}_{2-x}\text{O}_4$ increased with the decrease in the Rb^+ content (layer charge density), presumably due to the weaker electrostatic interactions between the interlayer Rb ions and the titanate sheets.

Recently, Okamoto *et al.* and we have investigated the synthesis of a series of $\text{K}_x\text{Ti}_{2-x/3}\text{Li}_{x/3}\text{O}_4$ to control the layer charge density.^{40, 41} Even when the ratio of Li_2CO_3 , K_2CO_3 , and TiO_2 in the solid-state reaction varied, a single phase product was obtained only at $x = \text{ca. } 0.80$ in $\text{K}_x\text{Ti}_{2-x/3}\text{Li}_{x/3}\text{O}_4$. However, by the post-synthetic treatment of $\text{K}_{0.78}\text{Ti}_{1.71}\text{Li}_{0.29}\text{O}_4$, which was obtained by the solid-state reaction, with aqueous H_2SO_4 followed by annealing, $\text{K}_x\text{Ti}_{2-y}\text{Li}_y\text{O}_4$ with different amounts of the interlayer K^+ ($x = 0.74, 0.67$, and 0.61) were obtained. The x value depends on the amounts of the added H_2SO_4 . The interlayer K^+ was then exchanged with Li^+ or Na^+ quantitatively, giving layered titanates with different composition ($\text{A}_x\text{Ti}_{2-y}\text{Li}_y\text{O}_4$, $\text{A} = \text{K}$ or Li ; Na ; $x = 0.61 - 0.76$).⁴² The water vapor adsorption and hydration in water were strongly influenced by the kind and amount of the interlayer cation, and the Na form with the smallest amount of the interlayer cation ($\text{Na}_x\text{Ti}_{2-y}\text{Li}_y\text{O}_4$, $x = 0.61$) was the best in terms of the degree of swelling (Fig. 4). Thus, the layer charge density of lepidocrocite-type layered titanates was successfully controlled to affect the properties by the post-synthetic treatment.

One can discuss the variation of CEC of smectites, which is in the range of 60-120 meq./100 g of clay, since the CEC value largely affect the performance of smectites. There are several ways of determining the layer charge density of smectites.¹⁰ The apparent CEC can be given by the contents of the interlayer cations, which was determined after all the interlayer cation was replaced with one kind of cation (so-called "homoionic-clay"). For this purpose, NH_4^+ and Ca^{2+} have often been used. Smectites are natural minerals, and even after the

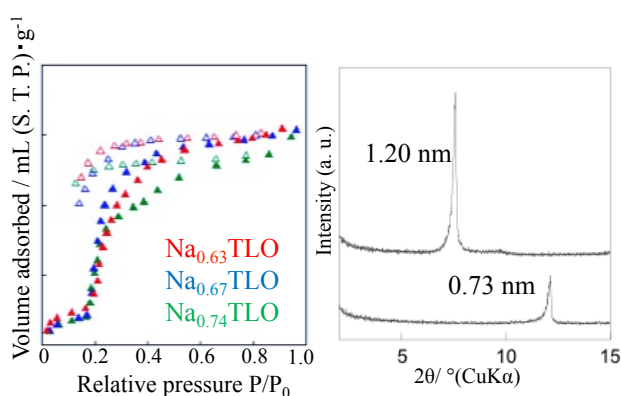


Fig. 4 Left: Water adsorption (filled symbol)/desorption (open symbol) isotherms of $\text{Na}_x\text{Ti}_{2-y}\text{Li}_y\text{O}_4$ [$x = 0.61$ (red filled/open triangle), 0.67 (blue filled/open triangle) and 0.76 (green filled/open triangle)]. Right: XRD patterns of $\text{Na}_{0.67}\text{Ti}_{2-y}\text{Li}_y\text{O}_4$ before (bottom) and after (top) the hydration.

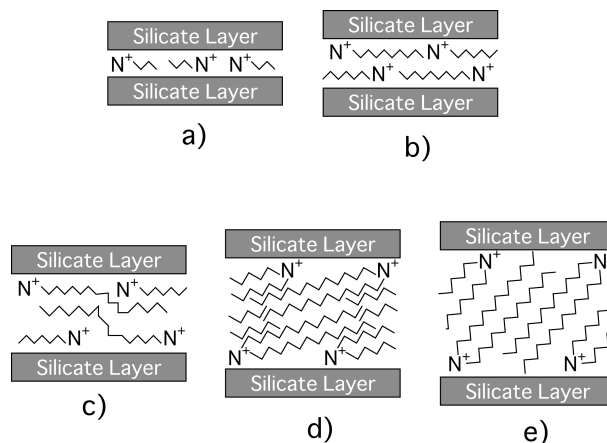


Fig. 5 Possible models for the arrangements of alkylammonium ions in smectites

purification, contain impurities, which affect the properties. The apparent CEC value (the unit is meq./100 g of clay) is based on the amount of clay with impurities. As a building block to construct desired nanostructure,⁴³ the comparison of CEC of pure smectite phase is more important. The CEC value of smectite portion (in this sense, layer charge density is more appropriate) is determined by the alkylammonium method.^{3, 44, 45} The alkylammonium methods are based on the quantitative ion exchange with alkylammonium ions with varied alkyl chain length and the structural transition from flat monolayer to bilayer and from bilayer to pseudo trimolecular layer was monitored by the expansion of the interlayer space as schematically shown in Fig. 5.⁴⁵

CEC is a direct measure to compare the difference of 2:1 type layered silicate, while as mentioned above, the content of the non-exchangeable impurity affects the CEC value. In addition, we need another unit to compare the CECs in a more general way, because various layered solids with different structure, composition and density are available. For this purpose, the layer charge density (charge per unit area), which means the available area for each valence as expressed in the unit of $\text{nm}^2 \text{ charge}^{-1}$, can be used. Layer charge density is determined based on the composition and the crystal structure and the values of various layered solids are summarized in Table 1 (adapted from Ref. 3, p.316 with modification).

Table 1. Layer charge densities of various layered materials

Compound	Area ($\text{nm}^2 \text{ Charge}^{-1}$)
Pyrophyllite / Talc	0
Smectites	0.40 - 1.20
$\text{Zr}(\text{HPO}_4)_2 \cdot \text{H}_2\text{O}$	0.24
$\text{KCa}_2\text{Nb}_3\text{O}_{10}$	0.30
KTiNbO_5	0.24
$\text{Na}_2\text{Ti}_3\text{O}_7$	0.17
$\text{K}_2\text{Ti}_4\text{O}_9$	0.23
$\text{A}_x\text{Ti}_{2-y}\text{M}_y\text{O}_4$ ($0.58 \leq x \leq 0.90$) A: K, Rb, Cs, M: Li, Co, Fe, etc.	0.25-0.38
Magadiite	0.26

The structure of long chain *n*-alkylammonium ion intercalated layered solids has been examined to determine the layer charge densities of various layered solids.^{7, 44} Being different from smectites, which have very low layer charge density (ca. 0.4 – 1.20 nm² charge⁻¹) so that the monolayer and bilayer arrangements of alkylammonium ions with their alkyl chains parallel to the silicate layer (the schematic structures are shown in Fig. 5) are possible, paraffin type arrangements of alkylammonium ions in the interlayer space are often observed and the inclination of the extended alkyl chain is a measure of the layer charge density; higher layer charge density results in the larger inclination of alkylammonium ions normal to the layer. More recently, alkylammonium ions with more complex structures, as shown in Fig. 6, have been used to be intercalated into layered silicates⁴⁶ as an alternative probe to evaluate the layer charge density. Amphiphilic dyes, where long-chain alkyl groups are attached to the chromophore, have also been used as guest species.⁴⁷⁻⁵⁰ A series of the amphiphilic azo dyes with variable alkyl chain lengths have been synthesized and the formation of self-assembled bilayer structures in aqueous solutions and in cast films has been examined.⁵¹ The molecular structures affect the orientation and the aggregation of the azobenzene chromophore in the bilayer structures, and the spectral properties are strongly affected by the microstructures. The orientation of the adsorbed dye cations (Fig. 6) was controlled by the host-guest interactions through complexation with smectites and other layered silicates.⁴⁷⁻⁵⁰ As an advantage of the amphiphilic dye, one can discuss the nanostructure from the visible absorption spectra of the intercalation compounds.

2-2. Effects of the spatial distribution of guest on the function of intercalation compounds

Smectites are the most widely investigated layered materials in the field of materials chemistry as they possess various attractive features such as the swelling behavior, ion-exchange properties, adsorptive properties, large surface area, *etc.*^{3, 8-10} Chemical and thermal stabilities as well as availability from nature, industry, and possible laboratory synthesis have led to research in a variety of fields taking advantage of the physics and chemistry of smectites. Here, we will discuss on the possible effects of the density and orientation of cationic guest species in the interlayer space on the properties of the products.

The replacement of the interlayer exchangeable cations with organoammonium ions results in the changes in the surface properties and the modified silicates have found application in the fields of the construction of novel host-guest systems where hydrophilic silicates do not have accessed.^{6, 52-54} When smectites are used as adsorbents, organic modification is often used to modify the chemical nature of the interlayer space to create the adsorbent for target adsorbates. Organoammonium modification can be classified roughly into two: one is organophilic modification and the other is pillaring as shown in Fig. 7.

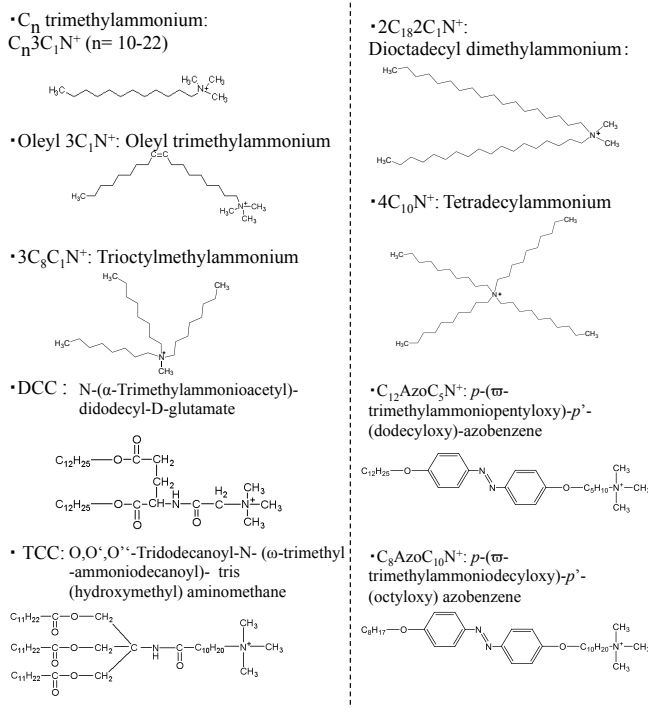


Fig. 6 Molecular structures of amphiphilic compounds used for the intercalation

The organic modification of smectites with small (non-amphiphilic) organoammonium cations has been investigated⁵⁵ for the adsorbents of toxic organic compounds. When small organic cations (*e.g.* tetramethylammonium ion) were used as pillars, the layer-charge density of smectites and the solvation of interlayer cations with water play important roles on possible size-exclusion effects. Adsorption of phenols and other organic compounds on organically pillared smectites has been investigated⁵⁵⁻⁶⁴ from environmental purification viewpoints. Pore size and porosity are expected to be controlled by selecting pillaring agents.

The adsorptive properties of smectites modified with aromatic ammonium ions have been reported,^{65, 66} while the interactions between the interlayer aromatic ammonium ions

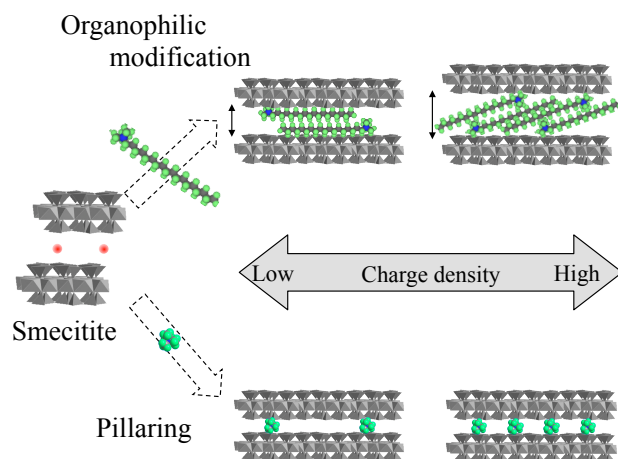


Fig. 7 Schematic drawings of two types of alkylammonium-smectites; the structures varied depending on the layer charge density of smectites

and organic non-ionic species to be adsorbed have scarcely been investigated. We have reported the adsorption behavior of phenols (phenol and 2,4-dichlorophenol) onto 1,1'-dimethyl-4,4'-bipyridinium (methylviologen: MV^{2+})-smectites from aqueous solution.⁶⁷ In order to show the possible role of layer charge density on the adsorption, a natural montmorillonite (Kunipia F; CEC of 119 meq./100 g of clay) and a synthetic saponite (Sumecton SA; CEC of 71 meq./100 g of clay) were used. The charge-transfer interactions between MV^{2+} and 2,4-dichlorophenol were thought to be a driving force for the adsorption as revealed by the color change in the MV^{2+} -saponite from colorless to yellow upon the adsorption of 2,4-dichlorophenol. The color-change signature upon the adsorption of a certain molecular species can probably be utilized as colorimetric sensing in a detector of environmental pollutants. Such a coloring reaction was also examined for MV^{2+} -modified synthetic clay minerals with controlled layer-charge density to show a possible role of MV^{2+} separation.¹² The adsorption of phenols (phenol and 2,4-dichlorophenol) from water on a natural montmorillonite (Kunipia F) and a synthetic saponite (Sumecton SA) modified with *p*-phenylenediammonium ions (abbreviated as PDA^{2+}) to obtain adsorbents with better performance (such as more obvious color change, greater adsorption capabilities and selective adsorption) was also studied.⁶⁸ Neostigmine, trimethylphenylammonium and 3-(trifluoromethyl) phenyltrimethylammonium were used to find the effects of the surface modification on the adsorption capacity of 2-phenylphenol, which is used for the post-harvest treatment of fruits and vegetables to protect against microbial damage during storage and distribution.⁶⁹ Among tested adsorbents, the neostigmine-modified smectites (Kunipia F, Sumecton SA and Tetrasilicic mica) effectively concentrate 2-phenylphenol from dilute aqueous solution and the largest adsorption capacity was obtained for neostigmine-modified Sumecton SA, which was ascribed to the largest pore volume due to the lowest surface layer charge density if compared with other two smectites. Even in the presence of sucrose, 2-phenylphenol was effectively adsorbed on the neostigmine-modified smectites.

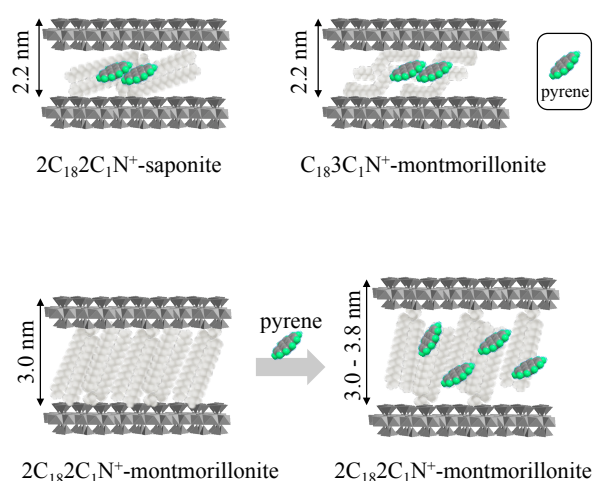


Fig. 8 Proposed difference in the states of pyrene intercalated in alkylammonium-smectites

The adsorption of phenols (phenol, 4-chlorophenol and 2,4-dichlorophenol) onto a natural montmorillonite (Kunipia F), a synthetic saponite (Sumecton SA) and a synthetic fluor-tetrasilicic mica (TSM) modified with tris(2,2'-bipyridine)ruthenium(II) (abbreviated as $[Ru(bpy)_3]^{2+}$) is another example to show the importance of the distance between adjacent cations on the molecular recognition.⁷⁰ The adsorption isotherms of phenol for the $[Ru(bpy)_3]^{2+}$ -clays from aqueous solution followed Langmuir type, indicating strong adsorbate-adsorbent interactions. The adsorption capacity of phenol varied depending upon the nature and one of the factors responsible for the variation in the adsorption capacity is the layer-charge density of smectites. Synthetic saponite (Sumecton SA; CEC of 71 meq./100 g of clay) led to a large pore volume in the interlayer space.

In addition to microporous organically pillared smectites, the organophilic smectites, which are obtained by the ion exchange with long-chain alkylammonium ions, have been applied to adsorb organic compounds (both cationic and nonionic) from environments.^{55, 58, 71-74} The adsorption of benzene, perchloroethene and 1,2-dichlorobenzene into hexadecyltrimethylammonium (abbreviated as $C_{16}3C_1N^+$)-clays from water has been investigated. The clay type affects the adsorption characteristics. The $C_{16}3C_1N^+$ -clays with larger amount of $C_{16}3C_1N^+$ showed better sorption capability. Greater adsorption capacity of alkylbenzenes (ethyl-, propyl- and butyl-benzenes) has been observed for the high layer charge $C_{16}3C_1N^+$ -clays.

Besides the adsorption capacity, the states of the adsorbed species have been affected by the layer charge density. Aromatic hydrocarbons such as pyrene have been used as luminescence probe of polarity and microviscosity in a variety of organized assemblies. Pyrene luminescence has been utilized to probe surfactant-modified smectites (Fig. 8). Upon solid-state reaction of octadecyltrimethylammonium($C_{18}3C_1N^+$)-montmorillonite and pyrene, a new d_{001} diffraction peak at ~ 3.7 nm appears, and the intensity of the d_{001} diffraction peak due to unreacted $C_{18}3C_1N^+$ -montmorillonite decreases.^{75, 76} In contrast, the basal spacings increased gradually from 3.0 to 3.8 nm as a function of the added amount of pyrene. The photoluminescence spectra of these pyrene-intercalated compounds suggested that the adsorbed pyrene molecules are more isolated in the interlayer space of the $2C_{18}2C_1N^+$ -montmorillonite than in $C_{18}3C_1N^+$ -montmorillonite. In order to elucidate the differences in the adsorption states, synthetic saponite (Sumecton SA; CEC of 71 meq./100 g of clay) was used.⁷⁷ The $2C_{18}2C_1N^+$ -saponite has a smaller basal spacing (2.2 nm), indicating that the intercalated ions possibly arranged as a pseudo-trimolecular layer similar to that for $C_{18}3C_1N^+$ -montmorillonite. When pyrene was intercalated, the change in the fluorescence spectra as a function of the concentration was similar to that for $C_{18}3C_1N^+$ -montmorillonite. The photoluminescence spectrum showed a tendency for pyrene molecules to form excimers (or dimers) similar to those for the $C_{18}3C_1N^+$ -montmorillonite and TSM systems. These facts suggested that the arrangements of the interlayer

alkylammonium ions largely affect the states of the adsorbed species. If the cations are oriented parallel to the silicate layers, adsorbed arenes tend to aggregate. Alkylammonium-smectites with the paraffin-type arrangement tend to solubilize the hydrocarbons molecularly.

Photoresponsive adsorbent, which shows reversible adsorption/desorption triggered by irradiation, has been reported. We have reported reversible change in the basal spacing by phenol adsorption triggered by photoirradiation. This was achieved by the complexation of smectite with a cationic azo dye, *p*-[2-(2-hydroxyethyl)dimethylammonio]ethoxy]azobenzene abbreviated as AZ⁺.^{50, 78, 79} Azobenzene is a well-known photochromic dye, which shows reversible *trans*-to-*cis* photoisomerization by UV irradiation and subsequent visible light irradiation or thermal treatment. Phenol was intercalated into AZ⁺ modified Kunipia F, whose cation exchange capacity (CEC) is 119 meq./ 100 g of clay, to expand the interlayer space by mechanical mixing. From the change in the XRD pattern (Fig. 9), photoinduced intercalation of phenol was observed by the UV irradiation, and subsequent visible light irradiation indicated phenol deintercalation. It was assumed that the intercalation and deintercalation of phenol induced by reversible *trans*-to-*cis* isomerization of the intercalated AZ⁺. More polar nature of *cis*-AZ⁺ possibly caused the intercalation of phenol. On the contrary, both of the intercalation and the photoinduced intercalation were not observed for the azo dye-Sumecton SA (the CEC of 71 meq./ 100 g of clay). The dye orientation with the molecular long axis inclined to the silicate layer plays an important role in the photoinduced intercalation of phenol.⁵⁰

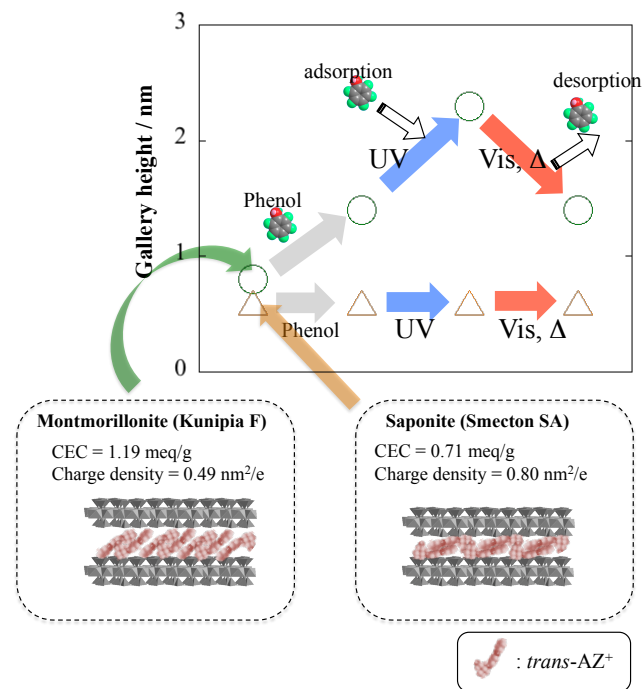


Fig. 9 Photoinduced intercalation of phenol into azobenzene modified-smectite occurred when the high layer charge smectites were used.

Beautiful examples of the controlled distance between two species on the clay mineral led to the controlled energy transfer was given by Margulies *et al.*^{80, 81} and Takagi *et al.*^{82, 83} The effect of the layer charge density (Takagi discussed the parameter as “intercharge distance”) of the clay on the complex formation behavior with cationic porphyrins has been carefully examined by Takagi *et al.* The maximum degrees of the adsorption for tetrakis(*N*-methylpyridinium-4-yl)porphyrin (H₂TMPyP⁴⁺) and tetrakis(*N,N,N*-trimethylanilinium-4-yl)porphyrin (H₂TMAP⁴⁺) were determined and the inter-cation distances are estimated to be 1.05 and 1.31 nm on the basis of calculations for H₂TMPyP⁴⁺ and H₂TMAP⁴⁺, respectively. The average intermolecular distances under the saturated adsorption condition were also estimated for the clay with different intercharge distance. The minimum intermolecular distance under the maximum adsorption condition depends upon the intramolecular charge distances of H₂TMPyP⁴⁺ (1.05 nm) and H₂TMAP⁴⁺ (1.31 nm). It is thus indicated that the high-density close packing of porphyrins on the clay surface takes place when the layer charge density on the clays matches well with the interpositive charge distance of the porphyrin molecule. Further discussion based on the systematic study can be found in a recent review articles.⁸⁴

Co-intercalation of photo- and catalytic-inactive species has been a way to isolate the active species and to provide a suitable nano-space for substrate/product selective reactions. For solid-acid catalyst, organoammonium ions were co-intercalated into acid-activated clays to tune the porosity and hydrophobicity of the interlayer space.⁸⁵ TMA modified acid-clay catalyzed isomerization of neat α -pinene to camphene selectively; the yield was higher when the C₁₂3C₁N⁺- and C₁₈3C₁N⁺-exchanged counterparts were used, and much higher than that of the simple acid-treated clay.

Regioselective photocycloaddition of stilbazolium cations in the interlayer space of saponite (Sumecton SA)⁸⁶ was shown by selective *syn* head-to-tail dimer formation upon irradiation. The states of γ -stilbazolium [4-(2-phenylvinyl)pyridinium] on Sumecton SA was successfully changed by the co-intercalation of alkylammonium ion as evidenced by the fact that the major photoreaction was changed from cyclodimerization to *E-Z* isomerization and the excimer emission of the intercalated stilbazolium ions was dramatically reduced.⁸⁷ The co-intercalation of C₁₆3C₁N⁺ suppressed the aggregation of Rhodamine 6G, showing light emitting ability for possible application to solid-state laser oscillator.⁸⁸

The spatial distribution of two kinds of cationic dyes is more complicated, since segregation may occur. Ghosh and Bard reported that smectite interlayer segregates [Ru(bpy)₃]²⁺ from exchangeable Na ions, resulting in high local concentrations of the complex ions in the interlayer space even at the low loading of [Ru(bpy)₃]²⁺ (only 1-2% of the CEC of Wyoming bentonite).⁸⁹ Dilution of [Ru(bpy)₃]²⁺ by the co-adsorption of [Zn(bpy)₃]²⁺ is one of the examples to control the separation of cations on smectites.⁸⁹ MV²⁺ ions are also segregated from [Ru(bpy)₃]²⁺. The co-intercalation of a water-soluble polymer is another way to control the state of cationic

dyes as well as the spatial distribution on smectites.⁹⁰⁻⁹⁵ The isolation of $[\text{Ru}(\text{bpy})_3]^{2+}$ has been achieved by the co-intercalation of poly(vinyl pyrrolidone) (abbreviated as PVP).^{90, 91} When $[\text{Ru}(\text{bpy})_3]^{2+}$ was intercalated in TSM without PVP, the diffraction peaks split into two, suggesting segregation. $[\text{Ru}(\text{bpy})_3]^{2+}$ was isolated effectively by PVP to suppress self-quenching even at higher concentration loading. It was suggested that co-intercalated PVP surrounds $[\text{Ru}(\text{bpy})_3]^{2+}$ in close contact in the sterically limited interlayer spaces to control the distance between adjacent $[\text{Ru}(\text{bpy})_3]^{2+}$.

Electron-transfer quenching of $[\text{Ru}(\text{bpy})_3]^{2+}$ by MV^{2+} in aqueous suspension of clays (Sumecton SA, Laponite XLG, and ME-100) in the presence of PVP was also investigated.⁹³ It has been known that MV^{2+} strongly interacts with clay surfaces and does not quench the excited state of $[\text{Ru}(\text{bpy})_3]^{2+}$ on clay due to segregation.⁸⁹ On the contrary, the adsorption of PVP on clay resulted in the co-adsorption of $[\text{Ru}(\text{bpy})_3]^{2+}$ and MV^{2+} without segregation.⁹³

Recently, the controlled expansion of the interlayer space (design the size of two-dimensional nanospace) was achieved by changing the adding PVP amount on synthetic saponite (Sumecton SA).⁹⁵ PVP was intercalated into Rhodamine 6G-Sumecton SA (0.1-1% of the CEC: 71 meq./100 g of clay) to investigate how the interlayer expansion affects the photoinduced event in the interlayer space. The interlayer expansion of Rhodamine 6G-clay varied linearly when PVP/clay weight ratio was lower than 3 (Fig. 10). The luminescence self-quenching efficiency varied depending upon the expansion of the interlayer space possibly due to the varied distance between the adjacent Rhodamine 6G (the distance correlated with the possibility of self-quenching).

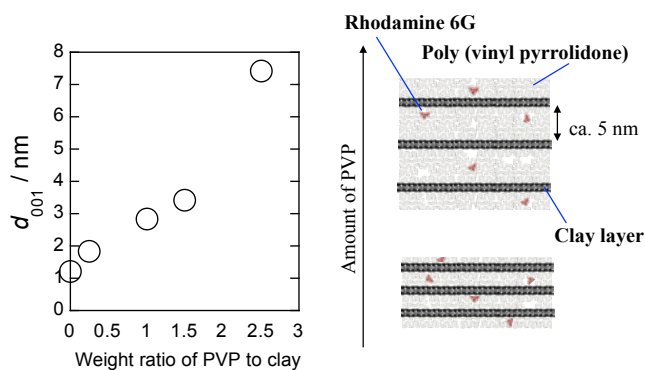


Fig. 10 Variation of the basal spacing of rhodamine 6G-smectite-poly(vinylpyrrolidone) intercalation compounds and the schematic drawings of the dilution (or separation) of rhodamine 6G intercalated in smectite by the intercalation of different amounts of poly(vinylpyrrolidone)

If compared with the modification with organoammonium ions, the polymer intercalation has advantages; the interlayer expansion can be controlled by the amount of polymer; for the organoammonium case, the amount cannot be used to control the expansion due to the segregation. In order to control the interlayer expansion, clays with different layer charge density^{11, 12, 96} or alkylammonium ions with different molecular structures

should be used. The use of polymers with varied molecular weight and branched structure is worth conducting to modify structure and property. Another advantage of the polymer intercalation is the improved stabilities of aqueous suspension and, as a result, optically transparent film can be obtained by drying the suspension on substrates. The films have also been prepared by means of alternate adsorption of a cationic polymer and the anionic sheet of an exfoliated clay.⁹⁷⁻¹⁰²

The limited and controlled swelling of lepidocrocite-type layered titanates is useful for molecular-sieve-like reactions. Ohtani *et al.* reported that $\text{H}_x\text{Ti}_{2-x/4}\square_{x/4}\text{O}_4$ ($x = 0.7$) exhibited a size-dependent decomposition of alcohols for H_2 production.¹⁰³ We have reported that $\text{Na}_x\text{Ti}_{2-y}\text{Li}_y\text{O}_4$ ($x = 0.61$) has such substrate selectivity in the photocatalytic decomposition as benzene was preferentially decomposed by UV light irradiation in the aqueous mixture over phenol and 4-butylphenol.⁴² The selectivity was thought to be due to access requirements for the interlayer space, namely, benzene was smaller than the gallery height (*ca.* 0.7 nm) of $\text{Na}_x\text{Ti}_{2-y}\text{Li}_y\text{O}_4$ ($x = 0.61$), thus benzene could effectively access the interlayer space to be decomposed. On the other hand, benzene was not intercalated into the K titanate, which did not swell, and was less effectively intercalated into the Li titanate, which has lower swelling ability than that of the Na form (Fig. 4).

3. Covalent attachments of functional units

Introducing organic functionality into the interlayer space of layered inorganic solids *via* covalent attachment is a useful way for the functionalization. Layered zirconium phosphonates, which are prepared by the reaction of zirconium salts and a variety of organophosphonates by a soft-solution process, are well-known examples of organically functionalized layered solids.¹⁰⁴⁻¹⁰⁶ On the other hand, the attachment of organic functionality to the interlayer space of pre-synthesized layered solids is also possible. Reactions between the interlayer silanol groups of layered silicates and silane coupling reagents became possible after pioneering work by Ruiz-Hitzky and Rojo.¹⁰⁷ Reactions between layered silicates and silane coupling agents have been summarized in a recent review.^{19, 108} Initially, the research was conducted to modify the surface silanol groups as much as possible, while the properties of the resulting hybrids have not been discussed. Later on, the degree of surface coverage with the grafted organic functionality is shown to affect the properties of the products (Fig. 11). Here, we will discuss the systems on the grafting of layered silicate and titanate.

We proposed that the distance between adjacent organic functional groups can be controlled to make nanospace accessible for guest species. Then, the distance has been controlled (0.52 - 0.66 nm; 0.28 - 0.44 nm^2 group⁻¹) by covalent attachment of semi-quantitative amounts of octylsilyl groups to layered silicate, magadiite.¹⁰⁹⁻¹¹¹ Alkyl alcohols were intercalated into the magadiites modified with controlled amounts of octylsilyl groups (0.44 nm^2 group⁻¹), while alkanes

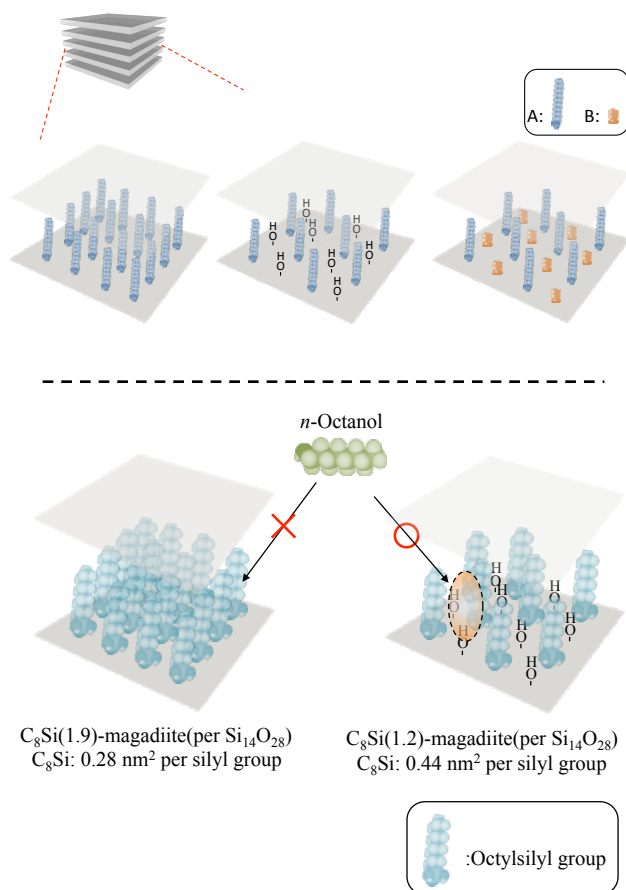


Fig. 11 Schematic drawings of possible variation of the spatial distribution of functional units grafted on layered inorganic solids

were not. These results have been explained as the cooperative effect of the geometry and the chemical nature of the surface covered with octyl groups and silanol groups. Not only the adsorption selectivity, the capacity for the uptake of alcohols was affected by the surface coverage (the distance between the adjacent functional groups). In the cases of the octylsilyl group modified magadiite, the interlayer expands by the uptake of alkylalcohols and the degree of the expansion was controlled by the alkyl chain length.

It has been shown that the surface coverage of organosilyl group affected their properties such as adsorptive one¹⁰⁹⁻¹¹¹ and swelling.¹¹²⁻¹¹⁵ The immobilization of controlled amounts of sulfonic acid groups on a layered sodium silicate, octosilicate, was also reported. The attachments of sulfonic acid groups on various porous materials has actively been done for possible application as catalysts¹¹⁶⁻¹¹⁹ and proton conductors,^{106, 120-124} while those on layered solids scarcely been reported.^{104, 105, 114, 125-127} The synthesis and application of the solid state proton conductor zirconium sulfophenyl phosphonate has been discussed.^{123, 124} The amounts (or the density) of sulfonic acid groups on the surface may affect the performance in applications. Once the modified layered silicate was exfoliated to be nanosheets, they can be regarded as platy nanoparticles covered with sulfonic acid groups. Octosilicate was modified first with the controlled amount of phenethyl group and the

immobilized phenethyl group was subsequently sulfonated by the reaction with chlorosulfonic acid.¹²⁸

The silylation of layered inorganic solids other than layered silicates has been investigated. Layered titanates ($K_2Ti_4O_9$ and KTLO) modified with octadecylsilyl groups have been prepared and the degree of surface coverage (0.44 - 0.87 nm^2 group⁻¹) are reported to affect the dispersion into organic solvents.¹¹⁵ As an example of more complex and sophisticated materials design, we have prepared $K_{0.80}Ti_{1.73}Li_{0.27}O_4$ modified with two different functional groups (octadecylsilyl and phenylsilyl groups) by the reaction of the dodecylammonium-exchanged $K_{0.80}Ti_{1.73}Li_{0.27}O_4$ with octadecyltrimethoxysilane and phenyltrimethoxysilane sequentially.¹²⁹ Two different guest tend to segregate, which is often observed for the adsorption of two cationic species in smectite clays.⁸⁹ However, judging from the X-ray diffraction pattern of the silylated $K_{0.80}Ti_{1.73}Li_{0.27}O_4$, the two functionalities were located in a same interlayer as schematically shown in Fig. 11. The silylated titanate effectively and selectively adsorbed 4-nonylphenol from the aqueous mixture with nonane and phenol. Since the silylated titanates in which one of the two functionalities were attached did not adsorb 4-nonylphenol effectively, the phenomenon observed on the octadecyl/phenyl groups-modified $K_{0.80}Ti_{1.73}Li_{0.27}O_4$ was explained by cooperative interactions of the attached octadecyl and phenyl groups (and silanol group derived from the hydrolysis of methoxy group) with nonyl and phenyl groups (and hydroxy group) of 4-nonylphenol.¹²⁹

We also examined the adsorption of 4-nonylphenol from an aqueous mixture of 4-butylphenol, 4-hexylphenol and 4-nonylphenol, which is difficult to be separated due to the structural similarity if compared with that of phenol, nonane and 4-nonylphenol, on a layered silicate (octosilicate) modified with the tuned amounts and ratios of octadecyl and phenyl groups.¹³⁰ Only the silylated octosilicate where the same ratios of octadecyl and phenyl groups were densely packed (0.36 nm^2 (silyl group)⁻¹) effectively and selectively adsorbed 4-nonylphenol from the aqueous mixture with 4-butylphenol and 4-hexylphenol. This result supported that the spatial distribution of octadecyl and phenyl (and silanol) groups on the titanate and silicate sheets was controlled. The expansion of the interlayer space of the silylated $K_{0.80}Ti_{1.73}Li_{0.27}O_4$ upon the 4-nonylphenol adsorption was larger than that of the silylated octosilicate; the variation in the swelling ability of the adsorbents was another possible factor.

The immobilization of two functionalities on a layer played a role to obtain polymer based nanocomposites.¹³¹⁻¹³³ We have reported the synthesis of a layered titanate-epoxy nanocomposite, where the titanate sheets were dispersed in the polymer, by the mixing of $K_{0.59}Ti_{1.66}Li_{0.34}O_4$ modified with octadecylsilyl and glycidylsilyl groups (0.33 nm^2 (silyl group)⁻¹) with epoxy resin followed by curing.¹³⁴ Since $K_{0.59}Ti_{1.66}Li_{0.34}O_4$ modified only with glycidylsilyl group did not form a nanocomposite when mixed with epoxy resin, it was indicated that the intercalation of an epoxy resin and copolymerization of the epoxy resin with the attached glycidyl

group were facilitated by the expansion of the interlayer space with the attachment of octadecyl group. Due to the swelling and precise surface modification, a lepidocrocite-type layered titanate was successfully embedded in an organic resin even by simple mixing. The nanocomposite exhibited durability toward UV light compared with the pristine epoxy resin. Moreover, the refractive index of the nanocomposite was controlled by the added amount of the organically modified titanate.

4. Hierarchically designed hybrid structure

Here, we will discuss hierarchically designed hybrid structures based on layered materials. As an example, hetero-nanosheets assembling of the exfoliated lepidocrocite-type layered titanate nanosheets has been conducted. Sasaki *et al.* have reported the successful formation of a sandwich system composed of negatively charged $\text{Ti}_{2-x/4}\square_{x/4}\text{O}_4$ nanosheets (or $\text{Ca}_2\text{Nb}_3\text{O}_{10}$ nanosheets derived from $\text{KCa}_2\text{Nb}_3\text{O}_{10}$) and positively charged $\text{Mg}_{0.67}\text{Al}_{0.33}(\text{OH})_2$ nanosheets, derived from the exfoliation of a layered double hydroxide (LDH), $\text{Mg}_{0.67}\text{Al}_{0.33}(\text{OH})_2 \cdot 0.17\text{CO}_3 \cdot 0.5\text{H}_2\text{O}$, by layer-by-layer deposition or simple flocculation.¹³⁵ Hwang *et al.* have reported a hetero-assembly of $\text{H}_x\text{Ti}_{2-x/4}\square_{x/4}\text{O}_4$ and $\text{Zn}_{0.69}\text{Cr}_{0.31}(\text{OH})_2 \cdot 0.31\text{NO}_3 \cdot 0.6\text{H}_2\text{O}$, which is known as an effective visible light-induced photocatalyst for O_2 production from water, by flocculation of the two exfoliated nanosheets.^{136, 137} The hybrid material showed higher photocatalytic O_2 production activity under visible light irradiation than pristine LDH, which was explained by the depression of electron-hole recombination rate of the LDH due to electron transfer from the LDH to the layered titanate upon the hybridization.

Mochizuki *et al.* have reported the formation of a hetero-assembly of $\text{H}_x\text{Ti}_{2-x/4}\square_{x/4}\text{O}_4$ and $\text{H}_2\text{W}_2\text{O}_7$ by a thiol-ene reaction between suspensions of $\text{H}_x\text{Ti}_{2-x/4}\square_{x/4}\text{O}_4$ modified with allyltrimethoxysilane ailane.¹³⁸ Under UV irradiation, the hybrid showed photocatalytic decomposition activity toward aqueous methylene blue higher than that of pristine layered titanate and tungstate, which was due to the effective charge separation.

Layered solids pillared with metal chalcogenides, represented by microporous Al_2O_3 - or ZrO_2 -pillared clays, have been widely investigated as catalysts and catalyst supports.¹³⁹ Pillared clays are usually prepared by the ion exchange of the interlayer cations of clays with bulky hydroxy metal cations such as $[\text{Al}_{13}\text{O}_4(\text{OH})_{13}]^{7+}$ and $[\text{Zr}_4(\text{OH})_{14}]^{2+}$, which are then converted to the oxide pillars on heating. Landis *et al.* developed a method to introduce pillar precursors into $\text{Na}_2\text{Ti}_3\text{O}_7$ by the pre-swelling with alkylammonium ions.¹⁴⁰ Yamanaka *et al.* reported the synthesis of SiO_2 -pillared $\text{Rb}_x\text{Mn}_x\text{Ti}_{2-x}\text{O}_4$ ($x = 0.75$) according to the procedure by Landis *et al.*¹⁴¹ By changing the alkyl chain length (C_n ; $n = 6 - 18$) of the intermediate, microporous materials with controlled pore volume were successfully prepared. SiO_2 -pillared $\text{Rb}_x\text{Mn}_x\text{Ti}_{2-x}\text{O}_4$ prepared from the hexylammonium-exchanged titanate

showed shape selectivity; the adsorption capacities of toluene or mesitylene vapors were considerably smaller than those of water or methanol vapors. The catalytic activity for the oxidation of CO with O_2 over SiO_2 -pillared $\text{Rb}_x\text{Mn}_x\text{Ti}_{2-x}\text{O}_4$ loaded with various metal cations (Cu, Co, Mn, Ni and Zn) was also investigated.¹⁴² SiO_2 -pillared $\text{Rb}_x\text{Mn}_x\text{Ti}_{2-x}\text{O}_4$ loaded with Cu showed the highest activity among the metal loaded samples. The high catalytic activity of the Cu-loaded sample was explained as a result of the porosity. In addition, the charge transfer between Cu and manganese titanate sheets was proposed; two redox reactions $\text{Cu}^{2+} \rightleftharpoons \text{Cu}^{1+}$ and $\text{Mn}^{3+} \rightleftharpoons \text{Mn}^{4+}$ played an important role for catalytic CO oxidation.

Kooli *et al.* applied the exfoliation/restacking of $\text{H}_x\text{Ti}_{2-x/4}\square_{x/4}\text{O}_4$ to prepare the mesoporous pillared titanate.^{143, 144} Mixing the suspension of exfoliated $\text{H}_x\text{Ti}_{2-x/4}\square_{x/4}\text{O}_4$ nanosheets and a solution of $[\text{Al}_{13}\text{O}_4(\text{OH})_{13}]^{7+}$ produced a pillared structure associated with double layers of Al_{13} cations, which was converted to a mesoporous Al_2O_3 -pillared titanate by subsequent heating. The surface area of the mesoporous pillared titanate was much higher than those of microporous pillared titanates prepared using the tetrabutylammonium- or hexylammonium-exchanged $\text{H}_x\text{Ti}_{2-x/4}\square_{x/4}\text{O}_4$ as the intermediate.¹⁴⁵

Choy, Hwang *et al.* have reported the synthesis and properties of a series of porous assemblies of lepidocrocite-type layered titanate nanosheets pillared with metal chalcogenides.¹⁴⁶⁻¹⁵³ Reassembling of exfoliated $\text{H}_{0.67}\text{Ti}_{1.83}\square_{0.17}\text{O}_4$ nanosheets with positively charged nickel hydroxide cluster followed by calcination resulted in a mesoporous NiO-pillared $\text{H}_{0.67}\text{Ti}_{1.83}\square_{0.17}\text{O}_4$.¹⁴⁸ The hybrid material showed catalytic activity for selective cyclohexane epoxidation. The selectivity and efficiency for desired cyclohexene oxide production was higher than those reported for other heterogeneous catalytic systems ever reported. The porous structure with many catalytically active sites was a possible reason for the high catalytic performance. Moreover, the hybrid material photocatalytically decomposed aqueous 4-chlorophenol under visible light irradiation due to the visible light harvesting of narrow-band gap NiO.

Recently, Hwang *et al.* have reported the highly efficient visible-light-induced H_2 generation from water on CdS nanoparticle (2.5 nm) incorporated in a mesoporous assembly of $\text{H}_{0.67}\text{Ti}_{1.83}\square_{0.17}\text{O}_4$ (with tetrabutylammonium cation), which was synthesized by mixing a $\text{H}_{0.67}\text{Ti}_{1.83}\square_{0.17}\text{O}_4$ nanosheets suspension with an acidic solution of CdS nanoparticle capped with 2-aminoethanethiol.¹⁴⁸ It should be noted that the H_2 -generated rate of the obtained co-catalyst-free hybrid material was greater than previously reported values for Pt-loaded CdS- TiO_2 hybrid systems. The hybrid showed the absorption edge red-shifted from that of the pristine titanate as a result of the complexation with visible-light-absorbing CdS, and the band gap energy of the hybrid was lower than that of the precursor CdS. The observed decrease of bandgap energy in the hybrid possibly resulted from strong electronic coupling between the two components, which allowed an efficient electron transfer from the valence band of the CdS to the conduction band

(and/or indirect bands) of the titanate and then gave efficient photocatalytic activity even without any co-catalyst.¹⁵³

In order to achieve steady H₂ evolution by the dye-sensitized layered semiconductor photocatalysts, an internally platinized layered niobate, Pt(in)/H₄Nb₆O₁₇, was applied as an n-type semiconductor instead of Pt/TiO₂.¹⁵⁴⁻¹⁵⁹ It has been demonstrated that the use of Pt(in)/H₄Nb₆O₁₇, where Pt nanoparticles are loaded in the interlayer spaces, is effective to suppress the undesirable backward reaction, i.e., rereduction of I₃⁻ to I⁻ on Pt. Since I₃⁻ anions are unable to access the Pt particles inside due to the electrostatic repulsion between the anionic I₃⁻ and the negatively charged (Nb₆O₁₇)⁴⁻ layers, the backward reduction of I₃⁻ to I⁻ can be effectively suppressed. When Pt cocatalysts were loaded both in the interlayers and on the external surface of H₄Nb₆O₁₇, the rate of H₂ evolution gradually decreased due to the occurrence of backward reduction of I₃⁻ on the Pt particles at the external surface.

Metallic nanoparticle have been synthesized in the clay interlayers as possible catalyst.¹⁶⁰ We have synthesized K_{0.66}Ti_{1.73}Li_{0.27}O₄ containing disc-like gold nanoparticle (named AuMPS_x-TLO) with the thickness less than 1 nm by the reaction of the mercaptopropylsilylated K_{0.66}Ti_{1.73}Li_{0.27}O₄ (MPS_x-TLO, where *x* denotes the amount (groups) of the attached alkylthiol per a unit cell of K_{0.66}Ti_{1.73}Li_{0.27}O₄) with HAuCl₄ followed by the reduction with NaBH₄ (Fig. 12).¹⁶¹⁻¹⁶³ The external surface was modified with octadecyl group to avoid the gold crystallization on the external surface and the interlayer thiol groups promoted the formation of gold nanoparticles preferentially in the interlayer through the strong interactions between nanoparticle surface and thiol group.

By changing the surface coverage with alkanethiol on the titanate nanosheet (1.1 nm² (silyl group)⁻¹ for *x* = 0.2; 0.45 nm² (silyl group)⁻¹ for *x* = 0.5), the thickness, diameter and spatial distribution of gold nanoparticle were successfully controlled (Fig. 12). The variation in the structure of AuMPS_x-TLO was reflected by the adsorption of a probe molecule, *o*-nitrophenol,

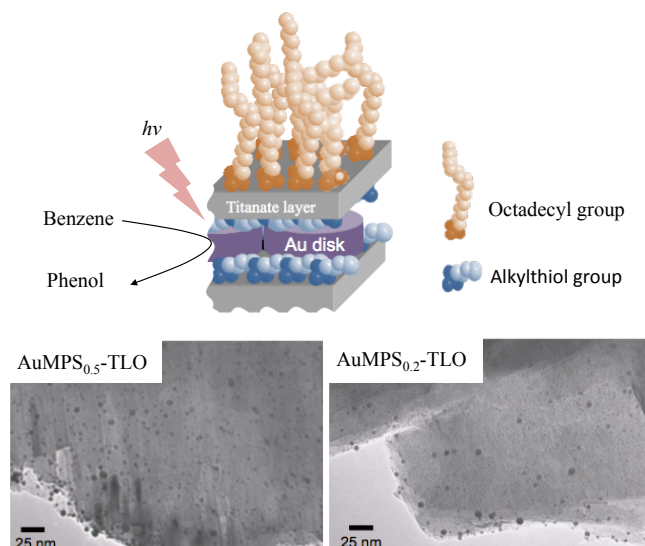


Fig. 12 Top: Schematic drawing of gold nanoparticles supported in the interlayer space of K_{0.66}Ti_{1.73}Li_{0.27}O₄. Bottom: the corresponding TEM images.

which is known to be adsorbed from water on zeolites and aminated polymers via the interactions with the surface hydroxyl or amino group. AuMPS_{0.2}-TLO with larger sized interlayer pore (due to thicker and smaller gold nanoparticle and longer inter-gold nanoparticle distance) and larger amount of the surface titanol groups adsorbed larger amount of *o*-nitrophenol than AuMPS_{0.5}-TLO.

AuMPS_{0.5}-TLO was used as a photocatalyst for direct benzene oxidation by visible light irradiation. It was found that AuMPS_{0.5}-TLO oxidized benzene in water to phenol under visible light and the yield and selectivity for phenol production (benzene base) substantially increased (up to 62% and 96%, respectively) depending on the amount of the added phenol in the starting mixture.

Oleic acid ligated magnetite nanoparticles have been immobilized on [H_{1-x}Ca₂Nb₃O₁₀]^{x-} modified with 3-aminopropyltrimethoxysilane, where the population of the magnetite particles varied depending on the synthetic conditions.¹⁶⁴

We have shown an example of topologically designed hybrid nanostructure composed of titania nanoparticles and dye-clay intercalate as dye-sensitized photocatalyst.^{165, 166} Superior stability of [Ru(bpy)₃]²⁺ for [Ru(bpy)₃]²⁺-saponite@TiO₂ if compared with that of an analogous ruthenium polypyridine complex (tris(2,2'-bipyridyl-4,4'-dicarboxylic acid) ruthenium(II) dichloride, abbreviated as Ru470) attached on the surface of a commercially available TiO₂ P25 (AEROXIDE[®] TiO₂ P25, Nippon Aerosil Co., Ltd.). This was achieved probably by the fact that [Ru(bpy)₃]²⁺ was separated from the semiconductor surface by clay nanosheet while at the same time photoexcited complex can be communicated with the semiconductor due to the hybrid structure schematically shown in Fig. 13. [Ru(bpy)₃]²⁺-saponite intercalation compound was coated with titania nanoparticles by a hydrothermal reaction of titanium tetraisopropoxide to obtain hybrid composed of anatase and clay. [Ru(bpy)₃]²⁺-saponite@TiO₂ was also prepared by mixing anatase sol with [Ru(bpy)₃]²⁺-saponite as thin film.

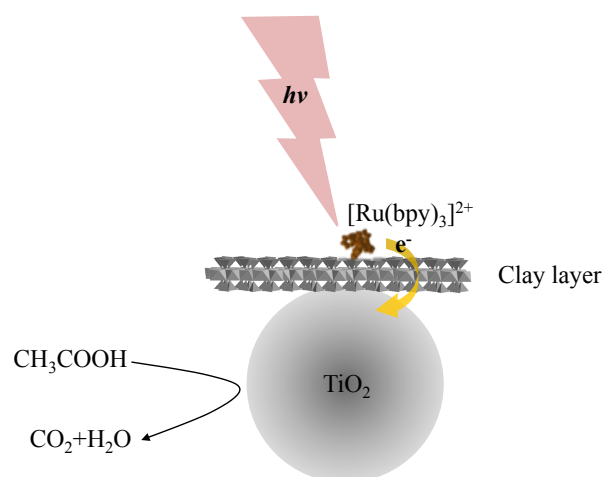


Fig. 13 Schematic model for the [Ru(bpy)₃]²⁺-smectite-TiO₂ hybrid; a visible light responsive photocatalyst

Taking advantage of the in-plane anisotropy of $K_4Nb_6O_{17}$, we have successfully constructed supramolecular structures with three-dimensional anisotropy. Cationic dyes were adsorbed on single crystals of $K_4Nb_6O_{17}$ and the orientations of the dyes were revealed by polarized spectra.^{167, 168}

5. Conclusions and future perspectives

The spatial distribution of functional units in the intercalation compounds has been controlled to optimize the performance. Layer charge density is a key to control the spatial distribution of cationic species, so that layered solids with different layer charge density has been used. Layer charge has been controlled intentionally and also designed. It has been also possible to modify the distance between adjacent functional units by the co-intercalation. Thanks to the expandable interlayer space, one can use various species to tune the nanostructure. The controlled spatial distribution of covalently attached organic functionality has been achieved by careful choice of synthetic conditions (sequence and quantity). Due to the controlled nanostructures, molecular selective adsorption or substrate/product selective reactions became available. Such photoinduced phenomena as photoinduced adsorption, photoinduced electron/energy transfer have been observed and the reactions have been optimized by the controlled spatial distribution of photofunctional molecular species. In addition to the interlayer nanostructure design, hybrids with hierarchically designed junction of functional nanoparticles are topic of current interests. Taking advantages of the rapid progresses of nanochemistry and morphosyntheses of inorganic solids, as well as organic and polymer synthetic materials chemistry, the design will be more and more artistic and we will enjoy the materials chemistry further.

Acknowledgements

The present work was supported financially by Waseda University as special research projects (2013B-054 and 2013B-055).

Notes and references

^a Department of Earth Sciences, Waseda University, Nishiwaseda 1-6-1, Shinjuku-ku, Tokyo 169-8050, Japan. E-mail address of corresponding author: makoto@waseda.jp

^b Graduate School of Creative Science and Engineering, Waseda University, Nishiwaseda 1-6-1, Shinjuku-ku, Tokyo 169-8050, Japan

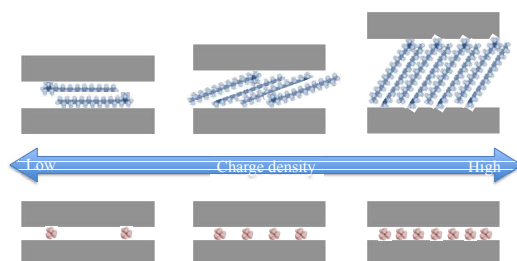
- M. Ogawa, *Annu. Rep. Prog. Chem. Sect., C: Phys. Chem.*, 1998, **94**, 209.
- Comprehensive Supramolecular Chemistry vol. 7*, ed. G. Alberti and T. Bein, Pergamon, Oxford, 1996.
- Handbook of Layered Materials*, ed. S. M. Auerbach, K. A. Carrado and P. K. Dutta, Taylor&Francis, Boca Raton, 2004.
- N. Kinomura, N. Kumada and F. Muto, *J. Chem. Soc.-Dalton Trans.*, 1985, 2349.
- M. Ogawa and K. Kuroda, *Chem. Rev.*, 1995, **95**, 399.
- M. Ogawa and K. Kuroda, *Bull. Chem. Soc. Jpn.*, 1997, **70**, 2593.
- G. Lagaly, *Solid State Ionics*, 1986, **22**, 43.
- Intercalation chemistry*, ed. M. S. Whittingham and A. J. Jacobson, Academic Press, 1982.
- Solid State Chemistry: Volume 2: Compounds*, eds. A. K. Cheetham and P. Day, Oxford University Press, USA, 1992, ch. 6.
- Handbook of Clay Science*, ed. F. Bergaya, B. K. G. Theng and G. Lagaly, Elsevier Science, Amsterdam, 2006.
- M. Ogawa, T. Matsutomo and T. Okada, *J. Ceram. Soc. Jpn.*, 2008, **116**, 1309.
- T. Okada, T. Matsutomo and M. Ogawa, *J. Phys. Chem. C*, 2010, **114**, 539.
- V. U. Hofmann and R. Klemen, *Z. Anorg. Chem.*, 1950, **262**, 95.
- R. Greenkelly, *Nature*, 1952, **170**, 1130.
- C. H. Lim and M. L. Jackson, *Clays Clay Miner.*, 1986, **34**, 346.
- K. Kitajima, F. Koyama and N. Takusagawa, *Bull. Chem. Soc. Jpn.*, 1985, **58**, 1325.
- W. J. Paulus, S. Komarneni and R. Roy, *Nature*, 1992, **357**, 571.
- G. Lagaly, *Adv. Colloid Interface Sci.*, 1979, **11**, 105.
- N. Takahashi and K. Kuroda, *J. Mater. Chem.*, 2011, **21**, 14336.
- M. Ogawa, Y. Ide and M. Mizushima, *Chem. Commun.*, 2010, **46**, 2241.
- S. Andersson and A. D. Wadsley, *Acta Chem. Scand.*, 1961, **15**, 663.
- S. Andersson and A. D. Wadsley, *Acta Crystallogr.*, 1961, **14**, 1245.
- A. Verbaere and M. Tournoux, *Bull. Soc. Chim. Fr.*, 1973, 1237.
- I. E. Grey, I. C. Madsen, J. A. Watts, L. A. Bursill and J. Kwiatkowska, *J. Solid State Chem.*, 1985, **58**, 350.
- A. F. Reid, W. G. Mumme and A. D. Wadley, *Acta Crystallogr.*, 1960, **B24**, 1228.
- M. Hervieu and B. Raveau, *Rev. Chim. Miner.*, 1981, **18**, 642.
- I. E. Grey, C. Li, I. C. Madsen, J. A. Watts and P. Melbourne, *J. Solid State Chem.*, 1987, **66**.
- T. Sasaki, Y. Komatsu and Y. Fujiki, *J. Chem. Soc.-Chem. Commun.*, 1991, 817.
- T. Sasaki, M. Watanabe, Y. Michiue, Y. Komatsu, F. Izumi and S. Takenouchi, *Chem. Mater.*, 1995, **7**, 1001.
- T. Sasaki, F. Izumi and M. Watanabe, *Chem. Mater.*, 1996, **8**, 777.
- T. Sasaki, M. Watanabe, H. Hashizume, H. Yamada and H. Nakazawa, *J. Am. Chem. Soc.*, 1996, **118**, 8329.
- T. Sasaki, Y. Ebina, Y. Kitami, M. Watanabe and T. Oikawa, *J. Phys. Chem. B*, 2001, **105**, 6116.
- M. Osada and T. Sasaki, *Adv. Mater.*, 2012, **24**, 210.
- T. Sasaki, F. Kooli, M. Iida, Y. Michiue, S. Takenouchi, Y. Yajima, F. Izumi, B. C. Chakoumakos and M. Watanabe, *Chem. Mater.*, 1998, **10**, 4123.
- T. Tanaka, Y. Ebina, K. Takada, K. Kurashima and T. Sasaki, *Chem. Mater.*, 2003, **15**, 3564.
- M. Osada, Y. Ebina, K. Fukuda, K. Ono, K. Takada, K. Yamaura, E. Takayama-Muromachi and T. Sasaki, *Phys. Rev. B*, 2006, **73**, 153301.
- M. Osada, Y. Ebina, K. Takada and T. Sasaki, *Adv. Mater.*, 2006, **18**, 295.
- M. Harada, T. Sasaki, Y. Ebina and M. Watanabe, *J. Photochem. Photobiol. A, Chem.*, 2002, **148**, 273.
- Z. L. Xu, K. Kunii, H. Fukuoka and S. Yamanaka, *Chem. Lett.*, 1999, 927.
- R. Hiroi, S. S. Ray, M. Okamoto and T. Shiroy, *Macromol. Rapid Commun.*, 2004, **25**, 1359.
- Y. Fuse, Y. Ide and M. Ogawa, *Bull. Chem. Soc. Jpn.*, 2008, **81**, 767.
- Y. Ide, Y. Nakasato and M. Ogawa, *J. Am. Chem. Soc.*, 2010, **132**, 3601.
- E. Ruiz-Hitzky, P. Aranda, M. Darder and M. Ogawa, *Chem. Soc. Rev.*, 2011, **40**, 801.
- G. Lagaly, *Clay Min.*, 1981, **16**, 1.
- P. T. Hang, *Clays Clay Miner.*, 1970, **18**, 203.
- M. Ogawa and D. Iwata, *Cryst. Growth Des.*, 2010, **10**, 2068.
- M. Ogawa, *Chem. Mater.*, 1996, **8**, 1347.
- M. Ogawa and A. Ishikawa, *J. Mater. Chem.*, 1998, **8**, 463.
- M. Ogawa, M. Yamamoto and K. Kuroda, *Clay Min.*, 2001, **36**, 263.
- T. Okada, Y. Watanabe and M. Ogawa, *J. Mater. Chem.*, 2005, **15**, 987.
- M. Shimomura, S. Aiba, N. Tajima, N. Inoue and K. Okuyama, *Langmuir*, 1995, **11**, 969.

52. *The Chemistry of Clay–Organic Reactions*, B. K. G. Theng, John Wiley & Sons Inc., London, 1974.
53. J. W. Jordan, B. J. Hook and C. M. Finlayson, *J. Phys. Colloid Chem.*, 1950, **54**, 1196.
54. T. R. Jones, *Clay Min.*, 1983, **18**, 399.
55. M. M. Mortland, S. Shaobai and S. A. Boyd, *Clays Clay Miner.*, 1986, **34**, 581.
56. R. M. Barrer, *Clays Clay Miner.*, 1989, **37**, 385.
57. Y. Park, G. A. Ayoko and R. L. Frost, *J. Colloid Interface Sci.*, 2011, **354**, 292.
58. S. A. Boyd, S. Shaobai, J. F. Lee and M. M. Mortland, *Clays Clay Miner.*, 1988, **36**, 125.
59. J. F. Lee, M. M. Mortland, S. A. Boyd and C. T. Chiou, *J. Chem. Soc. Faraday Trans. I*, 1989, **85**, 2953.
60. M. A. M. Lawrence, R. K. Kukkadapu and S. A. Boyd, *Appl. Clay Sci.*, 1998, **13**, 13.
61. Y. G. Yan and T. Bein, *Chem. Mater.*, 1993, **5**, 905.
62. J. A. Smith and P. R. Jaffe, *Environ. Sci. Technol.*, 1991, **25**, 2054.
63. Y. Seki, T. Okada and M. Ogawa, *Micropor. Mesopor. Mater.*, 2009, **124**, 30.
64. R. K. Kukkadapu and S. A. Boyd, *Clays Clay Miner.*, 1995, **43**, 318.
65. W. F. Jaynes and G. F. Vance, *Clays Clay Miner.*, 1999, **47**, 358.
66. S. Nir, T. Undabeytia, D. Yaron-Marcovich, Y. El-Nahhal, T. Polubesova, C. Serban, G. Rytwo, G. Lagaly and B. Rubin, *Environ. Sci. Technol.*, 2000, **34**, 1269.
67. T. Okada and M. Ogawa, *Chem. Commun.*, 2003, 1378.
68. T. Okada and M. Ogawa, *Bull. Chem. Soc. Jpn.*, 2004, **77**, 1165.
69. Y. Seki and M. Ogawa, *Bull. Chem. Soc. Jpn.*, 2010, **83**, 712.
70. T. Okada, T. Morita and M. Ogawa, *Appl. Clay Sci.*, 2005, **29**, 45.
71. S. A. Boyd, J. F. Lee and M. M. Mortland, *Nature*, 1988, **333**, 345.
72. W. F. Jaynes and S. A. Boyd, *Soil Sci. Soc. Am. J.*, 1991, **55**, 43.
73. S. A. Boyd, M. M. Mortland and C. T. Chiou, *Soil Sci. Soc. Am. J.*, 1988, **52**, 652.
74. J. A. Smith, P. R. Jaffé and C. T. Chlou, *Environ. Sci. Technol.*, 1990, **24**, 1167.
75. M. Ogawa, H. Shirai, K. Kuroda and C. Kato, *Clays Clay Miner.*, 1992, **40**, 485.
76. M. Ogawa, T. Aono, K. Kuroda and C. Kato, *Langmuir*, 1993, **9**, 1529.
77. M. Ogawa, T. Wada and K. Kuroda, *Langmuir*, 1995, **11**, 4598.
78. T. Okada, Y. Watanabe and M. Ogawa, *Chem. Commun.*, 2004, 320.
79. T. Okada, H. Sakai and M. Ogawa, *Appl. Clay Sci.*, 2008, **40**, 187.
80. L. Margulies, H. Rozen and E. Cohen, *Nature*, 1985, **315**, 658.
81. L. Margulies, H. Rozen and E. Cohen, *Clays Clay Miner.*, 1988, **36**, 159.
82. S. Takagi, D. A. Tryk and H. Inoue, *J. Phys. Chem. B*, 2002, **106**, 5455.
83. S. Takagi, T. Shimada, Y. Ishida, T. Fujimura, D. Masui, H. Tachibana, M. Eguchi and H. Inoue, *Langmuir*, 2013, **29**, 2108.
84. S. Takagi, M. Eguchi, D. A. Tryk and H. Inoue, *J. Photochem. Photobiol. C, Photochem. Rev.*, 2006, **7**, 104.
85. C. Breen, R. Watson, J. Madejová, P. Komadel and Z. Klapayta, *Langmuir*, 1997, **13**, 6473.
86. K. Takagi, H. Usami, H. Fukaya and Y. Sawaki, *J. Chem. Soc.-Chem. Commun.*, 1989, 1174.
87. H. Usami, K. Takagi and Y. Sawaki, *Bull. Chem. Soc. Jpn.*, 1991, **64**, 3395.
88. R. Sasai, N. Iyi, T. Fujita, F. L. Arbeloa, V. M. Martinez, K. Takagi and H. Itoh, *Langmuir*, 2004, **20**, 4715.
89. P. K. Ghosh and A. J. Bard, *J. Phys. Chem.*, 1984, **88**, 5519.
90. M. Ogawa, M. Inagaki, N. Kodama, K. Kuroda and C. Kato, *J. Phys. Chem.*, 1993, **97**, 3819.
91. M. Ogawa, M. Tsujimura and K. Kuroda, *Langmuir*, 2000, **16**, 4202.
92. H. Miyata, Y. Sugahara, K. Kuroda and C. Kato, *J. Chem. Soc. Faraday Trans. I*, 1987, **83**, 1851.
93. N. Kakegawa and M. Ogawa, *Langmuir*, 2004, **20**, 7004.
94. J. E. Martin, A. J. Patil, M. F. Butler and S. Mann, *Adv. Funct. Mater.*, 2011, **21**, 674.
95. M. Sohmiya, S. Omata and M. Ogawa, *Polym. Chem.*, 2012, **3**, 1069.
96. M. Ogawa, T. Matsutomo and T. Okada, *Bull. Chem. Soc. Jpn.*, 2009, **82**, 408.
97. E. R. Kleinfeld and G. S. Ferguson, *Science*, 1994, **265**, 370.
98. Y. Lvov, K. Ariga, I. Ichinose and T. Kunitake, *Langmuir*, 1996, **12**, 3038.
99. Z. Y. Tang, N. A. Kotov, S. Magonov and B. Ozturk, *Nat. Mater.*, 2003, **2**, 413.
100. T. Szabo, M. Szekeres, I. Dekany, C. Jackers, S. DeFeyter, C. T. Johnston and R. A. Schoonheydt, *J. Phys. Chem. C*, 2007, **111**, 12730.
101. B. V. Lotsch and G. A. Ozin, *Adv. Mater.*, 2008, **20**, 4079.
102. K. Ariga, Q. Ji, M. J. McShane, Y. M. Lvov, A. Vinu and J. P. Hill, *Chem. Mater.*, 2012, **24**, 728.
103. B. Ohtani, S. Ikeda, H. Nakayama and S. Nishimoto, *Phys. Chem. Chem. Phys.*, 2000, **2**, 5308.
104. G. Alberti, U. Costantino, S. Allulli and N. Tomassini, *J. Inorg. Nucl. Chem.*, 1978, **40**, 1113.
105. G. Alberti, U. Costantino, J. Környei and M. L. Luciani Giovagnotti, *React. Polym.*, 1985, **4**, 1.
106. G. Alberti, M. Casciola, U. Costantino and R. Vivani, *Adv. Mater.*, 1996, **8**, 291.
107. E. Ruiz-Hitzky and J. M. Rojo, *Nature*, 1980, **287**, 28.
108. T. Okada, Y. Ide and M. Ogawa, *Chem.-Asian J.*, 2012, **7**, 1980.
109. M. Ogawa, S. Okutomo and K. Kuroda, *J. Am. Chem. Soc.*, 1998, **120**, 7361.
110. I. Fujita, K. Kuroda and M. Ogawa, *Chem. Mater.*, 2003, **15**, 3134.
111. I. Fujita, K. Kuroda and M. Ogawa, *Chem. Mater.*, 2005, **17**, 3717.
112. Y. Ide and M. Ogawa, *Chem. Commun.*, 2003, 1262.
113. Y. Ide and M. Ogawa, *Chem. Lett.*, 2005, **34**, 360.
114. Y. Ide, G. Ozaki and M. Ogawa, *Langmuir*, 2009, **25**, 5276.
115. Y. Ide and M. Ogawa, *J. Colloid Interface Sci.*, 2006, **296**, 141.
116. W. M. Van Rhijn, D. E. De Vos, B. F. Sels, W. D. Bossaert and P. A. Jacobs, *Chem. Commun.*, 1998, 317.
117. M. H. Lim, C. F. Blanford and A. Stein, *Chem. Mater.*, 1998, **10**, 467.
118. J. A. Melero, R. van Grieken and G. Morales, *Chem. Rev.*, 2006, **106**, 3790.
119. M. Toda, A. Takagaki, M. Okamura, J. N. Kondo, S. Hayashi, K. Domen and M. Hara, *Nature*, 2005, **438**, 178.
120. M. Hara, T. Yoshida, A. Takagaki, T. Takata, J. N. Kondo, S. Hayashi and K. Domen, *Angew. Chem.-Int. Edit.*, 2004, **43**, 2955.
121. R. Marschall, J. Rathousky and M. Wark, *Chem. Mater.*, 2007, **19**, 6401.
122. J. B. Lee, Y. K. Park, O. B. Yang, Y. Kang, K. W. Jun, Y. J. Lee, H. Y. Kim, K. H. Lee and W. C. Choi, *J. Power Sources*, 2006, **158**, 1251.
123. G. Alberti, M. Casciola, U. Costantino, A. Peraio and T. Rega, *J. Mater. Chem.*, 1995, **5**, 1809.
124. G. Alberti, L. Boccali, M. Casciola, L. Massinelli and E. Montoneri, *Solid State Ionics*, 1996, **84**, 97.
125. P. M. Digiacomo and M. B. Dines, *Polyhedron*, 1982, **1**, 61.
126. C. Y. Yang and A. Clearfield, *React. Polym.*, 1987, **5**, 13.
127. J. L. Colon, C. Y. Yang, A. Clearfield and C. R. Martin, *J. Phys. Chem.*, 1988, **92**, 5777.
128. T. Nakamura and M. Ogawa, *Langmuir*, 2012, **28**, 7505.
129. Y. Ide and M. Ogawa, *Angew. Chem.-Int. Edit.*, 2007, **46**, 8449.
130. Y. Ide, S. Iwasaki and M. Ogawa, *Langmuir*, 2011, **27**, 2522.
131. *Polymer-Clay Nanocomposites*, ed. T. Pinnavaia and G. W. Beall, John Wiley & Sons Ltd., New York, 2001.
132. H. Heinz, *Clay Min.*, 2012, **47**, 205.
133. K. Isoda, K. Kuroda and M. Ogawa, *Chem. Mater.*, 2000, **12**, 1702.
134. Y. Fuse, Y. Ide and M. Ogawa, *Polym. Chem.*, 2010, **1**, 849.
135. L. Li, R. Z. Ma, Y. Ebina, K. Fukuda, K. Takada and T. Sasaki, *J. Am. Chem. Soc.*, 2007, **129**, 8000.
136. J. L. Gunjaker, T. W. Kim, H. N. Kim, I. Y. Kim and S. J. Hwang, *J. Am. Chem. Soc.*, 2011, **133**, 14998.
137. K. K. Manga, Y. Zhou, Y. L. Yan and K. P. Loh, *Adv. Funct. Mater.*, 2009, **19**, 3638.
138. D. Mochizuki, K. Kumagai, M. M. Maitani and Y. Wada, *Angew. Chem.-Int. Edit.*, 2012, **51**, 5452.
139. T. J. Pinnavaia, *Science*, 1983, **220**, 365.
140. M. E. Landis, B. A. Aufdembrink, P. Chu, I. D. Johnson, G. W. Kirker and M. K. Rubin, *J. Am. Chem. Soc.*, 1991, **113**, 3189.
141. S. Yamanaka, K. Kunii and Z. L. Xu, *Chem. Mater.*, 1998, **10**, 1931.
142. Z. L. Xu, K. Inumaru and S. Yamanaka, *Appl. Catal. A-Gen.*, 2001, **210**, 217.
143. F. Kooli, T. Sasaki and M. Watanabe, *Micropor. Mesopor. Mater.*, 1999, **28**, 495.
144. F. Kooli, T. Sasaki, V. Rives and M. Watanabe, *J. Mater. Chem.*, 2000, **10**, 497.

145. H. Jung, H. C. Lee, S. M. Paek, S. J. Hwang and J. H. Choy, *J. Phys. Chem. Solids*, 2006, **67**, 1248.
146. T. W. Kim, S. G. Hur, S. J. Hwang, H. Park, W. Choi and J. H. Choy, *Adv. Funct. Mater.*, 2007, **17**, 307.
147. T. W. Kim, S. J. Hwang, Y. Park, W. Choi and J. H. Choy, *J. Phys. Chem. C*, 2007, **111**, 1658.
148. T. W. Kim, S. J. Hwang, S. H. Jhung, J. S. Chang, H. Park, W. Choi and J. H. Choy, *Adv. Mater.*, 2008, **20**, 539.
149. T. W. Kim, H. W. Ha, M. J. Paek, S. H. Hyun, I. H. Baek, J. H. Choy and S. J. Hwang, *J. Phys. Chem. C*, 2008, **112**, 14853.
150. H. W. Ha, T. W. Kim, J. H. Choy and S. J. Hwang, *J. Phys. Chem. C*, 2009, **113**, 21941.
151. T. W. Kim, H. W. Ha, M. J. Paek, S. H. Hyun, J. H. Choy and S. J. Hwang, *J. Mater. Chem.*, 2010, **20**, 3238.
152. I. Y. Kim, K. Y. Lee, T. W. Kim and S. J. Hwang, *Mater. Lett.*, 2011, **65**, 894.
153. H. N. Kim, T. W. Kim, I. Y. Kim and S. J. Hwang, *Adv. Funct. Mater.*, 2011, **21**, 3111.
154. Y. I. Kim, S. Salim, M. J. Huq and T. E. Mallouk, *J. Am. Chem. Soc.*, 1991, **113**, 9561.
155. G. B. Saupe, T. E. Mallouk, W. Kim and R. H. Schmehl, *J. Phys. Chem. B*, 1997, **101**, 2508.
156. R. Abe, K. Sayama and H. Arakawa, *J. Photochem. Photobio. A, Chem.*, 2004, **166**, 115.
157. W. J. Youngblood, S. H. A. Lee, K. Maeda and T. E. Mallouk, *Acc. Chem. Res.*, 2009, **42**, 1966.
158. T. D. Nguyen-Phan, E. S. Oh, M. Chhowalla, T. Asefa and E. W. Shin, *J. Mater. Chem. A*, 2013, **1**, 7690.
159. R. Abe, K. Shinmei, N. Koumura, K. Hara and B. Ohtani, *J Am Chem Soc*, 2013, **135**, 16872.
160. P. B. Malla, P. Ravindranathan, S. Komarneni and R. Roy, *Nature*, 1991, **351**, 555.
161. Y. Ide, A. Fukuoka and M. Ogawa, *Chem. Mater.*, 2007, **19**, 964.
162. Y. Ide, Y. Nakasato and M. Ogawa, *Bull. Chem. Soc. Jpn.*, 2008, **81**, 757.
163. Y. Ide, M. Matsuoka and M. Ogawa, *J. Am. Chem. Soc.*, 2010, **132**, 16762.
164. F. E. Osterloh, *J. Am. Chem. Soc.*, 2002, **124**, 6248.
165. M. Ogawa, M. Sohmiya and Y. Watase, *Chem. Commun.*, 2011, **47**, 8602.
166. M. Ogawa and T. Goto, *Chem. Commun.*, 2014, submitted.
167. N. Miyamoto, K. Kuroda and M. Ogawa, *J. Am. Chem. Soc.*, 2001, **123**, 6949.
168. R. Kaito, K. Kuroda and M. Ogawa, *J. Phys. Chem. B*, 2003, **107**, 4043.

Table of contents

The effects of the spatial distribution of functional units in the interlayer space of intercalation compounds is discussed.



Highlight

The effects of the spatial distribution of functional units in the interlayer space of intercalation compounds is discussed. (19 words)